ACS APPLIED MATERIALS & INTERFACES

Research Article

www.acsami.org

Mesoporous Cerium Phosphonate Nanostructured Hybrid Spheres as Label-Free Hg^{2+} Fluorescent Probes

Yun-Pei Zhu,[†] Tian-Yi Ma,[†] Tie-Zhen Ren,[‡] and Zhong-Yong Yuan*,[†]

[†]Key Laboratory of Advanced Energy Materials Chemistry (Ministry of Education), Collaborative Innovation Center of Chemical Science and Engineering (Tianjin), College of Chemistry, Nankai University, Tianjin 300071, China

[‡]School of Chemical Engineering and Technology, Hebei University of Technology, Tianjin 300130, China

Supporting Information

ABSTRACT: Porous phosphonate-based organic–inorganic hybrid materials have been shown to have novel and amazing physicochemical properties due to the integration of superiorities from both inorganic components and organic moieties. Herein, mesoporous cerium phosphonate nanostructured hybrid spheres are prepared with the assistance of cationic surfactant cetyltrimethylammonium bromide while using ethylene diamine tetra(methylene phosphonic acid) as the coupling molecule. The resulting hybrid is constructed from the cerium phosphonate nanoparticles, accompanied by high specific surface area of 455 m^2 g^{-1}. The uniform incorporation of rare-earth element cerium and organophosphonic functionalities endows mesoporous cerium phosphonate with excellent fluorescence properties for the development of an optical sensor for selective Hg^{2+} detection on the basis of the fluorescence-quenching mechanism. The signal response of mesoporous cerium phosphonate against the Hg^{2+} concentration is linear over the range from 0.05 to 1.5 μmol L^{-1}, giving a limit of detection of 16 nmol L^{-1} (at a signal-to-noise ratio of 3). Most of the common physiologically relevant cations and anions did not interfere with the detection of Hg^{2+}. This label-free system provides a promising platform for further use in bioimaging and biomedical fields.

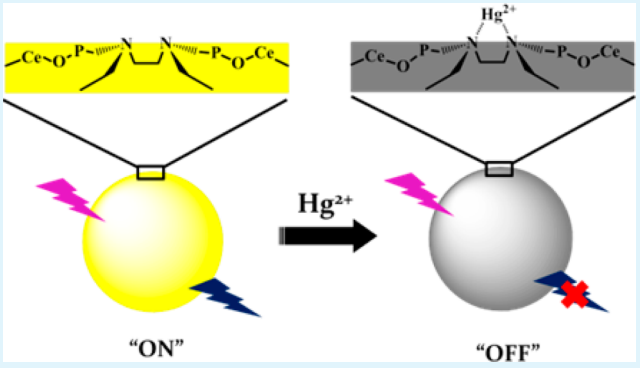

KEYWORDS: *cerium phosphonate, mesoporosity, fluorescence quenching, Hg^{2+} detection, sensor*

1. INTRODUCTION

By combining the virtues of materials science and nanotechnology, nanomaterials have aroused intense research interest in sensing detection of proteins, nucleic acids, and small molecules due to their peculiar optical, electronic, and catalytic properties.[1−4] Significantly, tremendous recent attention has been turned toward the rational design of nanomaterial-based sensors based on interactions between guest species and host nanomaterials with diverse compositions, dimensions, and morphologies.[5−8] With the increasing consideration of healthiness and sustainable environment, efficient detection of heavy transition-metal ions is a significant issue throughout the world because of the high toxicity. The mercury ion (Hg^{2+}) is ranked among the highly toxic metal ions and considered as one of the most dangerous and ubiquitous contaminants. There is a need to design an effective probe to detect Hg^{2+} at a low concentration in water. However, various drawbacks of the specific nanomaterials prohibit the application potential for detecting Hg^{2+}. Nanostructured carbons including carbon dots,[9,10] carbon nanotubes,[11] fullerene,[12] and graphene oxide[13] have been investigated as Hg^{2+} sensing platforms, wherein the carbon-related sensors are designed on the basis of their capability to quench previously labeled fluorescent probes, suggesting that the complicated process of fluorescent dye labeling and multistep chemical modifications are indispensable during the general measurements. On the other hand, as efficient fluorophores and the most widely used nanomaterials in sensing research, semiconductor nanocrystals or quantum dots (QDs) are usually nondispersible in water, and surface modification by organic capping agents or biomolecules is required to achieve good water-solubility and to enhance their interaction with guest ions.[14,15] It should also be noteworthy that the classical QDs contain heavy metal elements such as Cd, Hg, and Pb, which inevitably present biotoxicity and can further result in pollution. Also, noble metal nanoclusters demonstrate the superiorities of high fluorescence efficiency and size-tunable emission,[16,17] though elaborate preparation and postmodification are needed to realize the desired emission efficiency and water solubility. As a result, it remains a great challenge to develop an environmental-friendly sensing system for Hg^{2+} detection that involves no fluorescence labeling and heavy/noble metals.

Metal phosphonate hybrid materials have been proven to be multifunctional across the areas of adsorption, catalysis,

Received: July 15, 2014
Accepted: August 28, 2014
Published: August 28, 2014

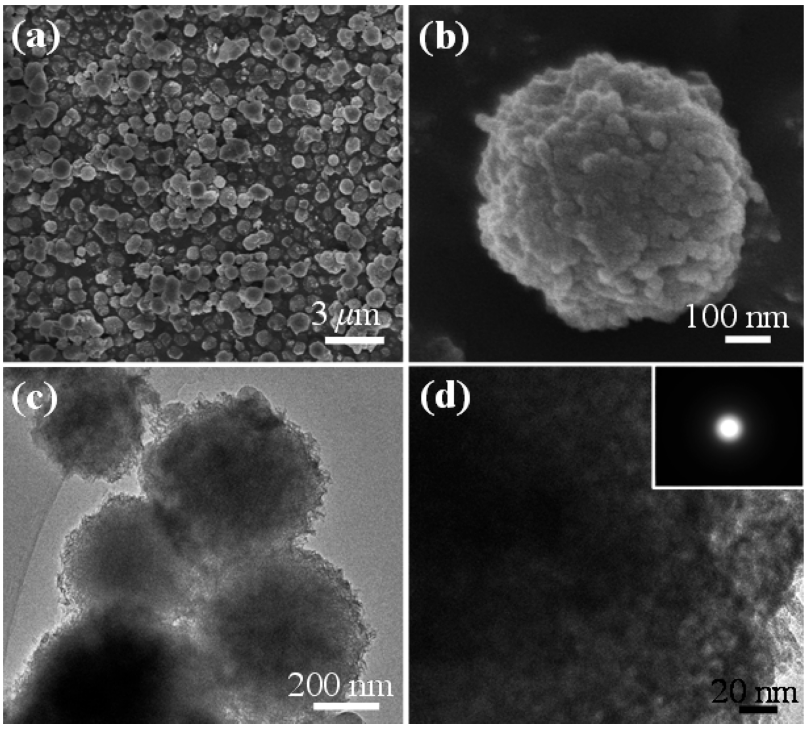

Figure 1. SEM (a, b) and TEM (c, d) images of the CeP-NS sample.

photoelectrochemistry, and bioapplications, due to the nearly infinite function modulation through judiciously changing the inorganic metallic units and organic phosphonic bridging groups in the homogeneous hybrid frameworks.[18−20] Mesoporous phosphonate-titania hybrid nanoparticles could perform as a bifunctional system for simultaneous bioresponsive sensing and controlled drug release, in which fluorescein labeled oligonucleotides were employed as the fluorescent probes.[21] Heavy metal ions can be efficiently removed from the wastewater by porous metal phosphonate hybrid adsorbents since the organic functionalities can supply interaction sites.[22,23] Nonetheless, metal phosphonates have rarely been used in direct metal ion sensing applications. Noticeably, much of the research on lanthanide phosphonates is targeting novel luminescence properties,[24,25] which renders them a great potential in optical sensing detection. However, one of the major constraints that needs to be tackled before the practical application is the congested porous structures,[24,26] resulting in limited interaction between host phosphonates and guest species. Although plentiful strategies have been taken to improve the resultant porosity including attaching additional functional groups on the organophosphonic linkages and utilizing secondary ligands,[18,24] the conventional complicated preparation makes them inconvenient and less cost-effective. Thus, a facile method is urgently required to prepare lanthanide phosphonates with well-structured porosity to cater to the ultimate detection purpose.

Herein, we report a surfactant-assisted approach to synthesize mesoporous cerium phosphonate nanostructured spheres using cationic surfactant cetyltrimethylammonium bromide (CTAB) and an polydentate claw molecule, ethylene diamine tetra(methylene phosphonic acid) (EDTMP). It is confirmed that the organophosphonic linkers are homogeneously immobilized in the mesoporous hybrid network, and the synthesized cerium phosphonate presents considerable photoluminescence and good dispersity in water. These attractive features endow the resulting cerium phosphoante with the applicability for constructing a sensing platform to detect highly toxic Hg^{2+}, and the excellent sensing is achieved by monitoring the fluorescence decay. This is the first report to explore metal phosphonates as detection systems to the best of our knowledge. The platform based on cerium phosphonate provides a promising alternative label-free and cost-effective sensing methodology.

2. EXPERIMENTAL SECTION

2.1. Synthesis of Mesoporous Cerium Phosphonate Nanostructured Spheres. In a typical synthesis procedure, EDTMP (0.001 mol) and CTAB (0.003 mol) were dissolved in 25 mL of deionized water, followed by stirring for 2 h at ambient temperature. $CeCl_3$ (0.002 mol) dissolved in 5 mL of deionized water was dropwise added into the mixed solution under vigorous stirring, and the pH value was adjusted by NaOH and HCl solution to be about 6.0 through the entire process. The mixture was kept at room temperature and stirred for another 2 h before being sealed in a Teflon-lined autoclave and aged statically at 120 °C under autogenous pressure for 24 h. The obtained product was filtered, washed with water repeatedly, and dried at 120 °C. The removal of the surfactant was accomplished by extracting the as-synthesized material (0.5 g) in ethanol (100 mL) with concentrated HCl (2 mL) for 20 h, and this process was repeated three times. The final material, mesoporous cerium phosphonate nanostructured spheres, was abbreviated as CeP-NS. In the meantime, cerium phosphonate nanoparticles, denoted as CeP-NP, were prepared in a similar procedure but in the absence of CTAB.

2.2. Fluorescence Test of Cerium Phosphonates in the Presence of Hg^{2+}. In a typical run, a 5 mmol L^{-1} stock solution of mercury nitrate was prepared, from which various Hg^{2+} concentrations were prepared by serial dilution. For fluorescence quenching studies, the interaction of cerium phosphonates and Hg^{2+} were conducted in Tris-HCl (pH 7.4) buffer solution under stirring at ambient conditions for 50 min before the spectra measurements. To evaluate the interaction kinetics between mesoporous cerium phosphonate and Hg^{2+}, the Hg^{2+} solution was mixed with mesoporous cerium

phosphonate, and then the time dependent fluorescence intensity was recorded.

2.3. Selectivity and Interference Measurements. To evaluate the selectivity of mesoporous cerium phosphonate, the following nitrate salts were utilized including K^+, Na^+, Mg^{2+}, Ca^{2+}, Sr^{2+}, Ba^{2+}, Zn^{2+}, Co^{2+}, Cd^{2+}, Cu^{2+}, and Pb^{2+}. In order to investigate possible anion interference in the mecury detection, the following sodium or potassium salts were used: F^-, Cl^-, NO_3^-, ClO_4^-, CH_3COO^-, $HCOO^-$, HPO_4^{2-}, SO_4^{2-}, and PO_4^{3-}. 1.0 mmol L^{-1} salt stock solutions were prepared. Subsequently, salt solutions of an appropriate volume were mixed with cerium phosphonates in the absence or presence of Hg^{2+}.

3. RESULTS AND DISCUSSION

3.1. Material Synthesis and Characterization. The synthesis of mesoporous cerium phosphonates nanostructured spheres was performed by the addition of cerium chloride into the aqueous solution of EDTMP in the presence of CTAB through a mild hydrothermal process. Removal of the surfactant was accomplished by extraction with acidic ethanol solution at a relatively low temperature to protect the organic–inorganic hybrid framework. The micromorphology is characterized by electron microscopy technique, as shown in Figure 1. Nanostructured spheres can be obviously seen with high yield in the SEM images (Figure 1a and b), of which the spherical diameter is in the range of 300–600 nm. TEM characterization confirms the well-defined porosity throughout the whole spheres (Figure 1c). By further magnifying the edge of a single nanostructured sphere (Figure 1d), wormhole-like holes that are aggregated by the cerium phosphonate nanoparticles are observed. The absence of lattice fringes from the observation of the high-magnification TEM image indicates the amorphous framework of cerium phosphonates, which is further confirmed by the selected area electron diffraction (SEAD) and wide-angle XRD patterns (Figure S1, Supporting Information). Distinctly, CeP-NP synthesized in the absence of surfactant is consisted of numerous nanoparticles, resulting in irregular micromorphology (Figure S2, Supporting Information). For the CeP-NS sample, one single and broad diffraction peak is present in the low-angle region (Figure S1, Supporting Information), suggestive of the presence of mesopores without long-range order.[27]

The textual properties of the synthesized hybrids were investigated by N_2 sorption analysis (Figure 2). The adsorption isotherm of CeP-NS is between type IV and type II, indicating

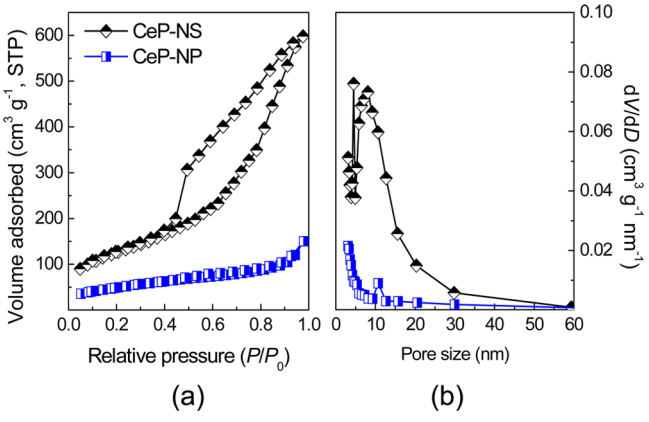

Figure 2. (a) N_2 adsorption–desorption isotherms of the synthesized cerium phosphonate materials and (b) the corresponding pore size distribution curves.

the existence of mesopores with good pore connectivity. In the desorption branch, the isotherm shows a hysteresis loop of type H2, indicative of ink-bottle-like pores that could be originated from the interparticle void spaces. The corresponding pore size distribution curve estimated by Barrett–Joyner–Halenda (BJH) model shows a distribution in the range of 3–30 nm. The specific surface area and pore volume are determined to be 455 $m^2\ g^{-1}$ and 0.93 $cm^{-3}\ g^{-1}$, respectively. However, as to the CeP-NP sample synthesized in the absence of surfactant, a typical isotherm of type III with a hysteresis loop of type H3 can be observed, and the measured surface area is 172 $m^2\ g^{-1}$ and pore volume is 0.24 $cm^3\ g^{-1}$. This signifies the positive role of the used surfactant species in enhancing the textual porosity of the final hybrid material. Mesoporous cerium phosphonates with high surface area have been seldom reported. The major reason may be due to the fact that the spherical ligating ability of simple organophosphonic acids would favor the formation of layered structures with the aryl or alkyl functional groups inhabited in the interlammellar spaces.[20,24,28] The limited interval between the organophosphonate pillars prevented the formation of accessible porosity. However, the unprecedented claw structures of EDTMP would perturb the general layered modes,[19,25] leading to the generation of amorphous cerium phosphonate nanoparticles, and the involvement of surfactant species would further improve the porous structures.

On the other side, organic surfactants can act as structure-directing agents and are extensively used to obtain nanostructured materials with various morphologies.[29−31] For instance, a diverse set of inorganic nanostructures with novel morphologies have been constructed with the aid of cationic CTAB.[32,33] In the present work, the positively charged cetyltrimethylammonium might tend to congregate and adhere on the negatively charged tetraorganophosphonic nanodrops based on the electrostatic attraction, leading to the generation of microphase-separated regions in the multiple component solution. A subsequent addition of cerium precursor would result in the reaction with phosphonic acid to form cerium phosphonate species, while cetyltrimethylammonium molecules kept wrapping the new-born phosphonates. The hydrothermal aging process would promote the adjacent capped cerium phosphonate nucleus to attach to each other to lower surface energy and form nearly spherical nanostructures by hydrophobic interaction and van der Waals attraction.[34,35] Accordingly, in the absence of cationic surfactant CTAB, the formed cerium phosphonate nanoparticles aggregated randomly and compactly, giving a relatively dense hybrid framework without well-structured morphology.

The skeletal structure of the mesoporous cerium phosphonate material was investigated by FT-IR spectrum and NMR. In the FT-IR spectra of CeP-NS (Figure 3), the broad band around 3400 cm^{-1} and the sharp band at 1652 cm^{-1} can correspond to the asymmetric OH stretching and bending vibration of the adsorbed water molecules.[36] The strong sharp band at 1075 cm^{-1} can be attributed to the P–O–Ce stretching vibrations, while the two bands at 473 and 571 cm^{-1} can be assigned to characteristic stretching vibrations of Ce–O bonds. The band at around 932 cm^{-1} assigned to the P–OH stretching vibrations cannot be observed, which reveals the extensive coordination with the cerium atoms, leading to mainly bidentate phosphonate units. The weak band at 1321 cm^{-1} can be attributed to the C–N stretching vibrations. The two weak bands at 1427 and 1462 cm^{-1}, corresponding to the C–H bending and P–C stretching modes of the methylphosphonic

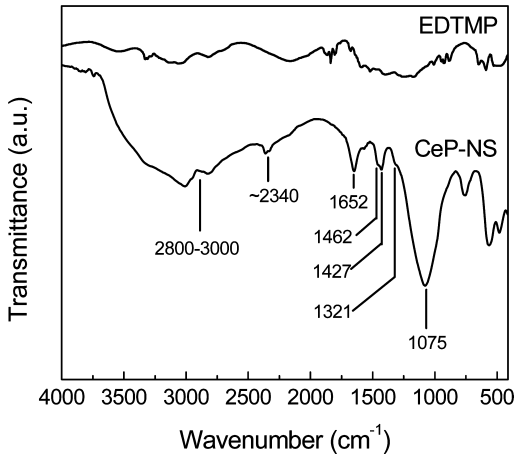

Figure 3. FT-IR spectra of pure EDTMP and the CeP-NS material.

moiety, can also be observed. The bands in the 2800−3000 cm^{-1} range correspond to the C−H stretching vibrations of the methylene carbon atoms in the organophosphonic ligands of the hybrids. The feature around 2340 cm^{-1} is typical of the antisymmetric stretching mode of pysisorbed CO_2 in the porous cerium phosphonate hybrid material.[37] The ^{31}P and ^{13}C MAS NMR spectra of the CeP-NS material are depicted in Figure S3, Supporting Information. One broad signal located at 10.2 ppm can be seen in the ^{31}P NMR spectrum, which is characteristic of metal phosphonates.[38] And the broadening of the resonance signal is due to the amorphous nature of solids, coinciding with SEAD and XRD analysis. No sharp ^{31}P NMR resonance signal at −4 ppm can be observed, indicating that layered phosphonate phases[23,39] are not presented in the present mesoporous cerium phosphonate material. Moreover, ^{13}C MAS NMR spectrum shows two major signals at 55.1 and 12.5 ppm, attributable to the carbon atoms in nitrilemethylenephosphonate groups and the bridging $-(CH_2)-$ groups, respectively.

High-resolution XPS were taken to illustrate the surface chemical state of CeP-NS (Figure 4). The XPS spectrum for

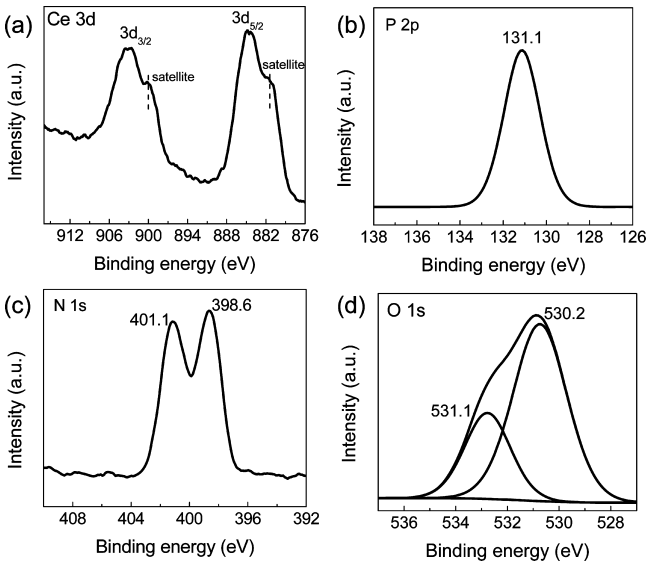

Figure 4. High-resolution XPS spectra of (a) Ce 3d, (b) P 2p, (c) N 1s, and (d) O 1s core levels in CeP-NS hybrid.

the Ce 3d core region is composed of two multiplets assigned to the spin−orbit split $3d_{5/2}$ and $3d_{3/2}$ separated by approximately 18.6 eV, while accompanied by two satellite peaks. This feature can be identified as the Ce^{3+} state in the cerium phosphonate material.[40,41] P 2p XPS spectra is symmetric with a maximum at binding energy of 131.1 eV, indicating the presence of exclusive P species, which is attributed to the P moieties in the organophosphonate ligands. The N 1s spectra shows twin peaks at around 398.6 and 401.1 eV, respectively, corresponding to the bridging N in the hybrid. Curve-fitting of the high-resolution spectrum of the O 1s asymmetric photoelectronic peak reveals that there are two kinds of oxygen. The main peak situated at 530.2 eV can be associated with the oxygen in the P−O−Ce linkages, and the other shoulder peak at 531.1 eV can be assigned to the existence of abundant surface hydroxyls or chemically adsorbed water molecules, thereby ensuring the good dispersity of CeP-NP in aqueous solution at a low concentration. The thermal stability of CeP-NS was determined by thermogravimetry and differential scanning calorimetry (TG−DSC) analysis. The TG curve in Figure S4, Supporting Information, shows an initial weight loss of 7.7% from room temperature to 205 °C accompanied by a shoulder endothermal peak at 72 °C that can be related to the desorption of physically adsorbed and intercalated water molecules. The weight loss of 12.5% in the region of 204−690 °C corresponds to the decomposition of organic species in the materials. The weight in the relatively high temperature range of 690 to 1000 °C resuls from the combustion of residual coke species. Hence the characterizations above suggest that organophisphonic moieties and cerium centers are homogeneously and tightly linked within the mesoporous cerium phosphonate hybrid framework.

3.2. Hg^{2+} Sensing. Mercury is a highly toxic element in ecosystems even at an extremely low concentration. Therefore, developing efficient methods to efficiently detect Hg^{2+} that allow sensitive and selective assays in aqueous media is in urgent demand. Numerous available techniques have been developed to detect the mercury level in the environment, such as high performance liquid chromatography, inductively coupled plasma atomic emission spectroscopy, and plasma mass spectroscopy.[42,43] But sophisticated instruments and sample treatments make these approaches time-consuming for data acquisition. By contrast, the fluorescent detection techniques for determination of metal ions are one of the best methods owing to the high sensitivity, portability, and low cost. Up to now, a number of systems such as semiconductor QDs,[36,44] noble metal nanocluster,[45,46] and some fluorophore-labeled systems[47,48] have been broadly investigated to monitor Hg^{2+} according to the fluorescence variation of the detection systems. We for the first time employ environmental-friendly mesoporous phosphonate-based hybrid materials as a sensing probe to establish a label-free fluorescent platform for Hg^{2+} detection.

The fluorescence emission spectra of the synthesized materials in the presence or absence of Hg^{2+} were recorded to evaluate the corresponding quenching ability. Figure 5 shows that the cerium phosphonates exhibit strong emission peaks centered at 352 nm, which can be ascribed to d−f transitions due to the spin−orbit splitting of the ground state of Ce^{3+}.[49,50] Remarkably, the CeP-NS material constructed from the aggregation of hybrid nanoparticles with well-developed mesoporosity and high surface area can significantly enhance the absorption efficiency of the excitation light and promote the

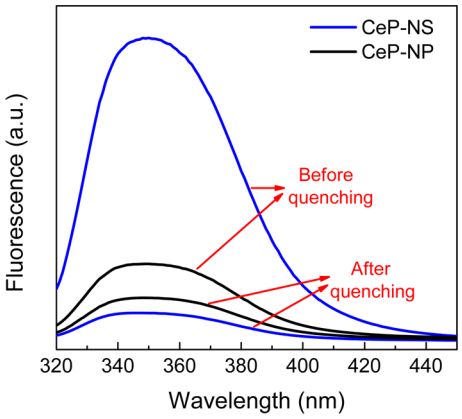

Figure 5. Fluorescence emission spectra of CeP-NS and CeP-NP before and after Hg^{2+} quenching (5 μmol L^{-1} Hg^{2+}, 30 μg mL^{-1} CeP-NS and CeP-NP, λ_{EX} = 300 nm).

quantum confinement effect,[51] which leads to much stronger fluorescence emission as compared to that of CeP-NP. For the CeP-NS sample, the quenching efficiency can be reached 90.3% upon interaction with 5 μmol L^{-1} Hg^{2+}, whereas only 56.4% quenching can be observed for CeP-NP, which can be due to the fact that mesoporous cerium phosphonate with preponderant porosity and much higher surface area provides abundant surface sites to interact with guest Hg^{2+} ions.

Moreover, the fluorescence quenching kinetics was investigated to find the suitable reaction time between Hg^{2+} and the cerium phosphonates (Figure 6). According to the experiment, the fluorescence intensity decreases gradually in the first 50 min and reaches equilibrium with further prolonging the reaction time. An optimal reaction time of 50 min was thus determined before the fluorescence measurement in this work. Considering the remarkable quenching effect of CeP-NS after the addition of Hg^{2+}, the possibility of exploiting a novel cerium-phosphonate-based fluorescence sensor for Hg^{2+} was then evaluated in detail. The fluorescence signal intensity is intimately dependent on the concentration of Hg^{2+} and can be analyzed using the Stern–Volmer equation:[52,53]

$$F_0/F = 1 + K_{SV}[Hg^{2+}]$$

where F_0 and F are the fluorescence intensity at 352 nm in the absence and presence of Hg^{2+}, respectively, K_{SV} represents the Stern–Volmer fluorescence quenching constant, which is a measurement of the quenching efficiency of the quencher, and $[Hg^{2+}]$ is the concentration of Hg^{2+}. The calibration curve in Figure 6b displays a good linear relationship (R^2 = 0.9901) of F_0/F versus $[Hg^{2+}]$ over the range from 0.05 to 1.5 μmol L^{-1}, accompanied by a K_{SV} = 3.28 × 10^6 L mol^{-1}. The limit of detection (LOD) of the cerium phosphonate nanostructured hybrid spheres for Hg^{2+} detection, calculated on the basis of the eq 3σ/slope (where σ is the standard deviation of the fluorescence intensity in the absence of metal ions), was 16 nmol L^{-1}, which is lower than the toxicity level of Hg^{2+} in drinking water (30 nmol L^{-1}) defined by World Health Organization (WHO). The present organic–inorganic hybrid probes more sensitive than that of state-of-the-art sensing systems reported to date in terms of LOD, i.e., fluorescent ssDNA-GO (30 nmol L^{-1}),[13] BSA-protected Au nanoclusters (80 nmol L^{-1}),[45] and cysteine-functionalized Ag nanoparticles (65 nmol L^{-1}).[54]

The fluorescence response of the CeP-NS in the presence of interferential metal ions was examined to test the selectivity of the present sensing platform. The corresponding fluorescence intensity variation of the CeP-NS toward a variety of common metal ions is shown in Figure 7a. Negligible interference upon the addition of Na^+, K^+, Mg^{2+}, Ca^{2+}, Sr^{2+}, Ba^{2+}, Zn^{2+}, Co^{2+}, Cd^{2+}, Pb^{2+}, and Cu^{2+} (with the same concentration as Hg^{2+}) can be observed implying that the fluorescent mesoporous cerium phosphonate material possess excellent selectivity toward Hg^{2+} sensing. On the other side, possible interference from common anions was investigated. Figure 7b demonstrates that there is little change in the emission in the presence of Hg^{2+} with the coexistence of 1.2 μmol L^{-1} F^-, Cl^-, NO_3^-, ClO_4^-, $HCOO^-$, CH_3COO^-, SO_4^{2-}, HPO_4^{2-}, and PO_4^{3-} as compared to that in the presence of single Hg^{2+}. These results suggest the potential applicability of the present mesoporous cerium phosphonate for the Hg^{2+} detection in real samples. Therefore, a novel and attractive label-free fluorescent sensing paltform for the detection of Hg^{2+} in the aqueous system has been developed on the basis of mesoporous cerium phosphoante hybrid nanostructured spheres.

With regard to the quenching mechanism, Foster resonance energy transfer (FRET) is ruled out because there is no spectrum overlap between the absorption of Hg^{2+} and the emission of cerium phosphonate (Figure S5, Supporting Information). XPS studies were further carried out on the Hg^{2+}-incorporated cerium phosphonate sample to illustrate the possible mechanism for such fluorescence quenching effect by Hg^{2+}. In comparison with the pristine CeP-NS, no significant changes in the C 1s and O 1s can be observed as to the Hg^{2+}-

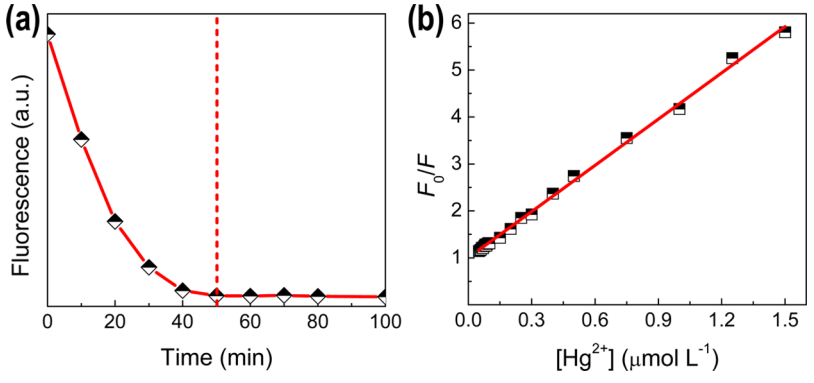

Figure 6. (a) Time-dependent fluorescence quenching of the CeP-NS fluorescent hybrid by Hg^{2+} (5 μmol L^{-1} Hg^{2+}, 30 μg mL^{-1} CeP-NS). (b) The titration plot of CeP-NS with Hg^{2+} in the concentration range from 0.05 to 1.5 μmol L^{-1}, showing a linear fit to the Stern–Volmer equation.

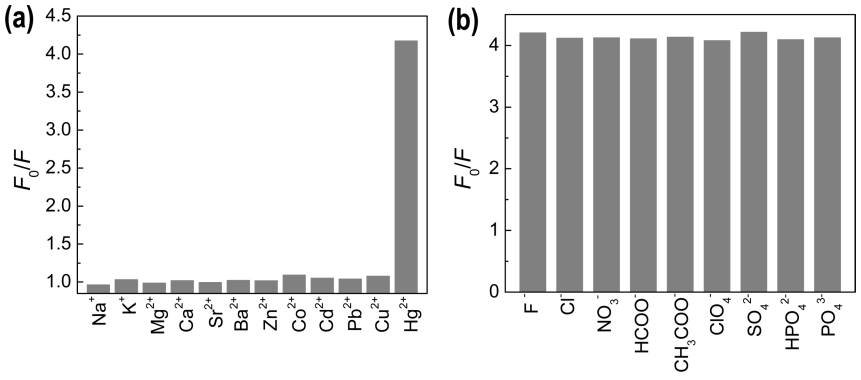

Figure 7. (a) Fluorescence quenching selectivity of CeP-NS toward different metal ions (30 μg mL^{-1} CeP-NS, 1.0 μmol L^{-1} metal ions). (b) Fluorescence response of CeP-NS with the coexistence of 1.2 μmol L^{-1} anions.

incorporated phosphonate sample (Figure S6, Supporting Information), which suggests the inappreciable interaction between Hg^{2+} ions and carbon, oxygen and phosphor atoms. However, the N 1s peaks of the nitrogen atoms are shifted to higher binding energy at 401.3 and 399.2 eV upon the addition of Hg^{2+}, revealing the substantial binding of the bridging nitrogen atoms in the phosphonate linkers to Hg^{2+}. Thus, static quenching might promote the decrease of fluorescence intensity owing to the formation of a stable nonfluorescent complex between CeP-NS and Hg^{2+}. Furthermore, the electron from cerium centers would transfer to the coordinated mercury ions due to the suitable redox potential of Hg^{2+}.[55,56] The occurrence of static quenching and electron transfer process would lead to the obvious decrease of fluorescence intensity. As the alkali (i.e., Na^+ and K^+) and alkaline-earth (i.e., Mg^{2+}, Ca^{2+}, Sr^{2+}, and Ba^{2+}) metal ions are not bound to the nitrogen atoms due to that pyridine-type nitrogen sites chemically immobilized on the hybrid framework show a selective sensing function with respect to the guest metal ions,[57,58] their influence on the fluorescent variation are negligible. The selectivity for Hg^{2+} toward fluorescence quenching of cerium phosphonate over other transition metal ions can be due to the relatively greater affinity of Hg^{2+} toward nitrogen atoms, larger ionic radius of Hg^{2+} and its capability to form an energetically favorable complex with cerium phosphonate,[59,60] as illustrated in Scheme 1.

The response of the CeP-NS hybrid material toward Hg^{2+} was found to be reversible. Upon the addition of Hg^{2+} chelating agent (disodium ethylenediamine tetraacetate, abbreviated as EDTA), the fluorescence could be effectively restored. After quenching by Hg^{2+}, the fluorescence of CeP-NS could return to 98.2% of the initial value when enough EDTA was added. Furthermore, the introduction of 5 μmol L^{-1} Hg^{2+} could lead to a quenching efficiency of about 90% for the recovered hybrid materials, suggesting the meaningful recoverability and reusability of the present fluorescent organic–inorganic hybrid detection systems. Although lanthanide-based metal–organic frameworks (MOFs) with valuable luminescent properties, which can be defined as crystalline organic–inorganic hybrids to some extent, have been gradually utilized as optical sensing materials.[61−63] Nevertheless, there are still some knotty problems. The major one is the insufficient water-solubility that restricts the further uses in biologic systems, and the emission band usually contains multipeaks, reducing the monochromaticity and measurement precision. Hence, the present mesoporous cerium phosphonate hybrid nanostructured spheres with well-defined porosity and good dispersity in water hold a promising potential for practical biosensing applications.

Scheme 1. Schematic Illustration of Hg^{2+} Detection by Mesoporous Cerium Phosphonate Nanostructured Spheres Based on Fluorescence-Quenching Mechanism

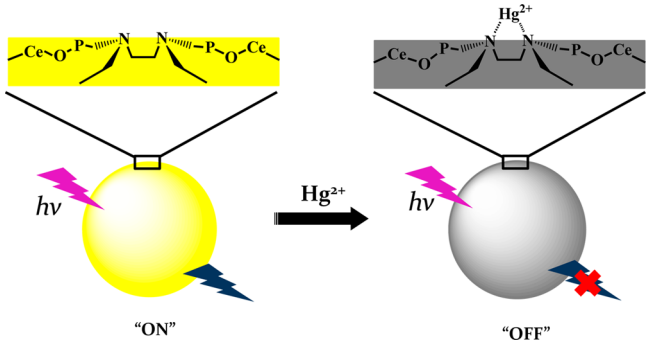

4. CONCLUSIONS

Mesoporous cerium phosphonate hybrid with well-structured micromorphology has been prepared through a facile hydrothermal method with the assistance of cationic surfactant. The spherical cerium phosphonate material that possessed high specific surface area is confirmed to consist of homogenesously linked inorganic cerium units and organophosphonic linkers. The resultant inherent photoluminescence property and organic functionalities make it a novel optimal platform for Hg^{2+} detection with excellent sensitivity and selectivity, and a limit of mercury ions detection of 16 nmol L^{-1} is determined. These results have an important significance for developing the applicable scope of lanthanide-based phosphonate fluorescent materials and structural sensors. We suggest that the label-free cerium phosphonates with promising biocompatibility can be used in research of new luminous materials in the areas of medical diagnostics, cell biology, and sensing devices for ion detection.

■ ASSOCIATED CONTENT

Supporting Information

Materials and characterization methods; SEM and TEM images of the CeP-NP sample; XRD patterns; ^{13}C and ^{31}P MAS NMR spectrum and TG-DSC curves of the CeP-NS material; UV–vis absorbance spectra of Hg^{2+} aqueous solution; high-resolution XPS spectrum of N 1s, C 1s, and O 1s for the Hg^{2+}-

incorporated CeP-NS sample. This material is available free of charge via the Internet at http://pubs.acs.org.

AUTHOR INFORMATION

Corresponding Author

*Fax +86 22 23502604. Tel +86 22 23509610. E-mail zyyuan@nankai.edu.cn.

Notes

The authors declare no competing financial interest.

ACKNOWLEDGMENTS

This work was supported by the National Natural Science Foundation of China (21073099), the Specialized Research Fund for the Doctoral Program of Higher Education (20110031110016), the Program for Innovative Research Team in University (IRT1059, IRT13022), the 111 project (B12015), the Key Laboratory of Advanced Catalytic Materials in Zhejiang Normal University (ZJHX201301), and the Ph.D. Candidate Research Innovation Fund of Nankai University.

REFERENCES

(1) Park, S. J.; Taton, T. A.; Mirkin, C. A. Array-Based Electrical Detection of DNA with Nanoparticle Probes. *Science* **2002**, *295*, 1503−1506.

(2) Fan, C. H.; Wang, S.; Hong, J. W.; Bazan, G. C.; Plaxco, K. W.; Heeger, A. J. Beyond Superquenching: Hyper-Efficient Energy Transfer From Conjugated Polymers to Gold Nanoparticles. *Proc. Natl. Acad. Sci. U.S.A.* **2003**, *100*, 6297−6301.

(3) Yang, H.; Xia, Y. N. Bionanotechnology: Enabling Biomedical Research with Nanomaterials. *Adv. Mater.* **2007**, *19*, 3085−3085.

(4) Zhang, X. L.; Zheng, C.; Guo, S. S.; Li, J.; Yang, H. H.; Chen, G. N. Turn-On Fluorescence Sensor for Intracellular Imaging of Glutathione Using g-C_3N_4 Nanosheet-MnO2 Sandwich Nanocomposite. *Anal. Chem.* **2014**, *86*, 3426−3434.

(5) Fan, W.; Lee, Y. H.; Pedireddy, S.; Zhang, Q.; Liu, T. X.; Ling, X. Y. Graphene Oxide and Shape-Controlled Silver Nanoparticle Hybrids for Ultrasensitive Single-Particle Surface-Enhanced Raman Scattering (SERS) Sensing. *Nanoscale* **2014**, *6*, 4843−4851.

(6) Darbha, G. K.; Ray, A.; Ray, P. C. Gold Nanoparticle-Based Miniaturized Nanomaterial Surface Energy Transfer Probe for Rapid and Ultrasensitive Detection of Mercury in Soil, Water, and Fish. *ACS Nano* **2007**, *1*, 208−214.

(7) Konvalina, G.; Haick, H. nsors for Breath Testing: From Nanomaterials to Comprehensive Disease Detection. *Acc. Chem. Res.* **2014**, *47*, 66−76.

(8) Zhang, J. F.; Park, M.; Ren, W. X.; Kim, Y.; Kim, S. J.; Jung, J. H.; Kim, J. S. A Pellet-Type Optical Nanomaterial of Silica-Based Naphthalimide-DPA-Cu(II) Complexes: Recyclable Fluorescence Detection of Pyrophosphate. *Chem. Commun.* **2011**, *47*, 3568−3570.

(9) Zhou, L.; Lin, Y. H.; Huang, Z. Z.; Ren, J. S.; Qu, X. G. Carbon Nanodots as Fluorescence Probes for Rapid, Sensitive, and Label-Free Detection of Hg^{2+} and Biothiols in Complex Matrices. *Chem. Commun.* **2012**, *48*, 1147−1149.

(10) Li, H. L.; Zhai, J. F.; Tian, J. Q.; Luo, Y. L.; Sun, X. P. Carbon Nanoparticle for Highly Sensitive and Selective Fluorescent Detection of Mercury(II) Ion in Aqueous Solution. *Biosens. Bioelectron.* **2011**, *26*, 4656−4660.

(11) Zhang, L. B.; Li, T.; Li, B. L.; Li, J.; Wang, E. K. Carbon Nanotube-DNA Hybrid Fluorescent Sensor for Sensitive and Selective Detection of Mercury(II) Ion. *Chem. Commun.* **2010**, *46*, 1476−1478.

(12) Li, H. L.; Zhai, J. F.; Sun, X. P. Nano-C-60 as A Novel, Effective Fluorescent Sensing Platform for Mercury(II) Ion Detection at Critical Sensitivity and Selectivity. *Nanoscale* **2011**, *3*, 2155−2157.

(13) He, S. J.; Song, B.; Li, D.; Zhu, C. F.; Qi, W. P.; Wen, Y. Q.; Wang, L. H.; Song, S. P.; FangH, P.; Fan, C. H. A Graphene Nanoprobe for Rapid, Sensitive, and Multicolor Fluorescent DNA Analysis. *Adv. Funct. Mater.* **2010**, *20*, 453−459.

(14) Paramanik, B.; Bhattacharyya, S.; Patra, A. Detection of Hg^{2+} and F^- Ions by Using Fluorescence Switching of Quantum Dots in an Au-Cluster-CdTe QD Nanocomposite. *Chem.—Eur. J.* **2013**, *19*, 5980−5987.

(15) Somers, R. C.; Bawendi, M. G.; Nocera, D. G. CdSe Nanocrystal Based Chem-/Bio-Sensors. *Chem. Soc. Rev.* **2007**, *36*, 579−591.

(16) Triulzi, R. C.; Micic, M.; Giordani, S.; Serry, M.; Chiou, W.; Leblanc, R. M. Immunoasssay Based on the Antibody-Conjugated PAMAM-Dendrimer-Gold Quantum Dot Complex. *Chem. Commun.* **2006**, 5068−5070.

(17) Huang, C. C.; Yang, Z.; Lee, K. H.; Chang, H. T. Synthesis of Highly Fluorescent Gold Nanoparticles for Sensing Mercury(II). *Angew. Chem., Int. Ed.* **2007**, *46*, 6824−6828.

(18) Zhu, Y. P.; Ren, T. Z.; Yuan, Z. Y. Mesoporous Non-Siliceous Inorganic-Organic Hybrids: A Promising Platform for Designing Multifunctional Materials. *New J. Chem.* **2014**, *38*, 1905−1922.

(19) Ma, T. Y.; Yuan, Z. Y. Metal Phosphonate Hybrid Mesostructures: Environmentally Friendly Multifunctional Materials for Clean Energy and Other Applications. *ChemSusChem* **2011**, *10*, 1407−1419.

(20) Gagnon, K. J.; Perry, H. P.; Clearfield, A. Conventional and Unconventional Metal-Organic Frameworks Based on Phosphonate Ligands: MOFs and UMOFs. *Chem. Rev.* **2012**, *112*, 1034−1054.

(21) Li, H.; Ma, T. Y.; Kong, D. M.; Yuan, Z. Y. Mesoporous Phosphonate-TiO_2 Nanoparticles for Simultaneous Bioresponsive Sensing and Controlled Drug Release. *Analyst* **2013**, *138*, 1084−1090.

(22) Zhu, Y. P.; Liu, Y. L.; Ren, T. Z.; Yuan, Z. Y. Mesoporous Nickel Phosphate/Phosphonate Hybrid Microspheres with Excellent Performance for Adsorption and Catalysis. *RSC Adv.* **2014**, *4*, 16018−16021.

(23) Ma, T. Y.; Lin, X. Z.; Yuan, Z. Y. Periodic Mesoporous Titanium Phosphonate Hybrid Materials. *J. Mater. Chem.* **2010**, *20*, 7406−7415.

(24) Mao, J. G. Structures and Luminescent Properties of Lanthanide Phosphonates. *Coord. Chem. Rev.* **2007**, *251*, 1493−1520.

(25) Shimizu, G. K. H.; Vaidhyanathan, R.; Taylor, J. M. Phosphonate and Sulfonate Metal Organic Frameworks. *Chem. Soc. Rev.* **2009**, *38*, 1430−1449.

(26) Ying, S. M.; Mao, J. G. Producing a Second Ligand: New Route to Luminescent Lanthanide Polyphosphonates. *Cryst. Growth Des.* **2006**, *6*, 964−968.

(27) Wang, X. C.; Yu, J. C.; Ho, C. M.; Hou, Y. D.; Fu, X. Z. Photocatalytic Activity of a Hierarchically Macro/Mesoporous Titania. *Langmuir* **2005**, *21*, 2552−2559.

(28) Clearfield, A. Organically Pillared Micro- and Mesoporous Materials. *Chem. Mater.* **1998**, *10*, 2801−2810.

(29) Ge, J. P.; Hu, Y. X.; Biasini, M.; Beyermann, W. P.; Yin, Y. D. Superparamagnetic Magnetite Colloidal Nanocrystal Clusters. *Angew. Chem., Int. Ed.* **2007**, *46*, 4342−4345.

(30) Voort, P. V. D.; Esquivel, D.; Canck, E. D.; Goethals, F.; Driessche, I. V.; Romero-Salgueroc, F. J. Periodic Mesoporous Organosilicas: From Simple to Complex Bridges; A Comprehensive Overview of Functions, Morphologies and Applications. *Chem. Soc. Rev.* **2013**, *42*, 3913−3955.

(31) Grzelczak, M.; Pérez-Juste, J.; Mulvaney, P.; Liz-Marzán, L. M. Shape Control in Gold Nanoparticle Synthesis. *Chem. Soc. Rev.* **2008**, *37*, 1783−1791.

(32) Kim, M. P.; Ku, K. H.; Kim, H. J.; Jang, S. G.; Yi, G. R.; Kim, B. J. Surface Intaglio Nanostructures on Microspheres of Gold-Cored Block Copolymer Spheres. *Chem. Mater.* **2013**, *25*, 4416−4422.

(33) Zhu, C.; Peng, H. C.; Zeng, J.; Liu, J.; Gu, Z.; Xia, Y. Facile Synthesis of Gold Wavy Nanowires and Investigation of Their Growth Mechanism. *J. Am. Chem. Soc.* **2012**, *134*, 20234−20237.

(34) Zhang, C.; Cheng, Z.; Yang, P.; Xu, Z.; Peng, C.; Li, G.; Lin, J. Architectures of Strontium Hydroxyapatite Microspheres: Solvothermal Synthesis and Luminescence Properties. *Langmuir* **2009**, *25*, 13591−13598.

(35) Cong, H. P.; Yu, S. H. Hybrid ZnO-Dye Hollow Spheres with New Optical Properties from a Self-Assembly Process Based on Evans Blue Dye and Cetyltrimethylammonium Bromide. *Adv. Funct. Mater.* **2007**, *17*, 1814−1820.
(36) Dutta, A.; Mondal, J.; Patra, A. K.; Bhaumik, A. Synthesis and Temperature-Induced Morphological Control in a Hybrid Porous Iron-Phosphonate Nanomaterial and Its Excellent Catalytic Activity in the Synthesis of Benzimidazoles. *Chem.—Eur. J.* **2012**, *18*, 13372−13378.
(37) Kauffman, K. L.; Culp, J. T.; Goodman, A.; Matranga, C. FT-IR Study of CO_2 Adsorption in a Dynamic Copper(II) Benzoate-Pyrazine Host with CO_2-CO_2 Interactions in the Adsorbed State. *J. Phys. Chem. C* **2011**, *115*, 1857−1866.
(38) Kimura, T. Synthesis of Mesostructured and Mesoporous Aluminum Organophosphonates Prepared by Using Diphosphonic Acids with Alkylene Groups. *Chem. Mater.* **2005**, *17*, 337−344.
(39) Guerrero, G.; Mutin, P. H.; Vioux, A. Mixed Nonhydrolytic/Hydrolytic Sol-Gel Routes to Novel Metal Oxide/Phosphonate Hybrids. *Chem. Mater.* **2000**, *12*, 1268−1272.
(40) Zhang, Y.; Wang, J.; Zhang, T. Novel Ca-Doped $CePO_4$ Supported Ruthenium Catalyst with Superior Catalytic Performance for Aerobic Oxidation of Alcohols. *Chem. Commun.* **2011**, *47*, 5307−5309.
(41) Kitsuda, M.; Fujihara, S. Quantitative Luminescence Switching in $CePO_4$:Tb by Redox Reactions. *J. Phys. Chem. C* **2011**, *115*, 8808−8815.
(42) Guo, Z.; Liu, Z. G.; Yao, X. Z.; Zhang, K. S.; Chen, X.; Liu, J. H.; Huang, X. J. A Molecular-Gap Device for Specific Determination of Mercury Ions. *Sci. Rep.* **2013**, *3*, 3115.
(43) Rastogi, L.; Sashidhar, R. B.; Karunasagar, D.; Arunachalam, J. Gum Kondagogu Reduced/Stabilized Silver Nanoparticles as Direct Colorimetric Sensor for the Sensitive Detection of Hg^{2+} in Aqueous System. *Talanta* **2014**, *118*, 111−117.
(44) Zhang, J.; Tian, J.; He, Y.; Zhao, Y.; Zhao, S. A K^+-Mediated G-Quadruplex Formation Enhancement Fluorescence Polarization System Based on Quantum Dots for Detection of Hg^{2+} and Biothiols. *Chem. Commun.* **2014**, *50*, 2049−2051.
(45) Hu, D.; Sheng, Z.; Gong, P.; Zhang, P.; Cai, L. Highly Selective Fluorescent Sensors for Hg^{2+} Based on Bovine Aerum Albumin-Capped Gold Nanoclusters. *Analyst* **2010**, *135*, 1411−1416.
(46) Ghosh, S.; Anand, U.; Mukherjee, S. Luminescent Silver Nanoclusters Acting as a Label-Free Photoswitch in Metal Ion Sensing. *Anal. Chem.* **2014**, *86*, 3188−3194.
(47) Wang, Q.; Wang, W.; Lei, J.; Xu, N.; Gao, F.; Ju, H. Fluorescence Quenching of Carbon Nitride Nanosheet through Its Interaction with DNA for Versatile Fluorescence Sensing. *Anal. Chem.* **2013**, *85*, 12182−12188.
(48) Zhang, Y.; Gao, L.; Wen, L.; Heng, L.; Song, Y. Highly Sensitive, Eelective and Reusable Mercury(II) Ion Sensor Based on A ssDNA-Functionalized Photonic Crystal Film. *Phys. Chem. Chem. Phys.* **2013**, *15*, 11943−11949.
(49) Li, Q.; Yam, V. W. W. Redox Luminescence Switch Based on Energy Transfer in $CePO_4$: Tb^{3+} Nanowires. *Angew. Chem., Int. Ed.* **2007**, *46*, 3486−3489.
(50) Kömpe, K.; Borchert, H.; Storz, J.; Lobo, A.; Adam, S.; Möller, T.; Haase, M. Green-Emitting $CePO_4$: Th/$LaPO_4$ Core-Shell Nanoparticles with 70% Photoluminescence Quantum Yield. *Angew. Chem., Int. Ed.* **2003**, *42*, 5513−5516.
(51) Alivisatos, A. P. Semiconductor Clusters, Nanocrystals, and Quantum Dots. *Science* **1996**, *271*, 933−937.
(52) Lakowicz, J. R. *Principles of Fluorescence Spectroscopy*; Kluwer Academic/Plenum Press: New York, 1999.
(53) Panchompoo, J.; Aldous, L.; Baker, M.; Wallace, M. I.; Compton, R. G. One-Step Synthesis of Fluorescein Modified Nano-Carbon for Pd(II) Detection via Fluorescence Quenching. *Analyst* **2012**, *137*, 2054−2062.
(54) Shang, L.; Yin, J.; Li, J.; Jin, L.; Dong, S. Gold Nanoparticle-Based Near-Infrared Fluorescent Detection of Biological Thiols in Human Plasma. *Biosens. Bioelectron.* **2009**, *25*, 269−274.
(55) Bünzli, J. C. G.; Piguet, C. Taking Advantage of Luminescent Lanthanide Ions. *Chem. Soc. Rev.* **2005**, *34*, 1048−1077.
(56) Duan, J.; Jiang, X.; Ni, S.; Yang, M.; Zhan, J. Facile Synthesis of N-acetyl-l-cysteine Capped ZnS Quantum Dots as an Eco-friendly Fluorescence Sensor for Hg^{2+}. *Talanta* **2011**, *85*, 1738−1743.
(57) Liu, S.; Xiang, Z.; Hu, Z.; Zheng, X.; Cao, D. Zeolitic Imidazolate Framework-8 as a Luminescent Material for the Sensing of Metal Ions and Small Molecules. *J. Mater. Chem.* **2011**, *21*, 6649−6653.
(58) Chen, B.; Wang, L.; Xiao, Y.; Fronczek, F. R.; Xue, M.; Cui, Y.; Qian, G. A Luminescent Metal-Organic Framework with Lewis Basic Pyridyl Sites for the Sensing of Metal Ions. *Angew. Chem., Int. Ed.* **2009**, *48*, 500−503.
(59) Barman, S.; Sadhukhan, M. Facile Bulk Production of Highly Blue Fluorescent Graphitic Carbon Nitride Quantum Dots and Their Application as Highly Selective and Sensitive Sensors for the Detection of Mercuric and Iodide Ions in Aqueous Media. *J. Mater. Chem.* **2012**, *22*, 21832−21837.
(60) Sadhukhan, M.; Barman, S. Bottom-Up Fabrication of Two-Dimensional Carbon Nitride and Highly Sensitive Electrochemical Sensors for Mercuric Ions. *J. Mater. Chem. A* **2013**, *1*, 2752−2756.
(61) Chen, B.; Wang, L.; Zapata, F.; Qian, G.; Lobkovsky, E. B. A Luminescent Microporous Metal-0Organic Framework for the Recognition and Sensing of Anions. *J. Am. Chem. Soc.* **2008**, *130*, 6718−6719.
(62) Zhu, X.; Zheng, H.; Wei, X.; Lin, Z.; Guo, L.; Qiu, B.; Chen, G. Metal-Organic Framework (MOF): A Novel Sensing Platform for Biomolecules. *Chem. Commun.* **2013**, *49*, 1276−1278.
(63) Luo, F. Batten, S. R. Metal-Organic Framework (MOF): Lanthanide(III)-Doped Approach for Luminescence Modulation and Luminescent Sensing. *Dalton Trans.* **2010**, *39*, 4485−4488.